Wideband LNA Noise Matching

Eugene Zailer, Leonid Belostotski *Member, IEEE*, and Rene Plume

***Abstract*—A new method for designing wideband noise- and power-matched source-degenerated cascode LNAs is presented. At the core of the method is the selection of transistor size and biasing that simultaneously minimize the difference between the LNA noise factor and the minimum noise factor as well as reduce the sensitivity of that difference to frequency. An experimental demonstration of the method is presented with a 0.13-µm CMOS LNA exhibiting <-12dB S11, 10dB of gain, and <2.5dB NF, which remains within 2.8% of the minimum noise figure, from 4 to 8GHz while consuming 12.8mW of power.**

***Index Terms*—Source-degenerated LNA, noise matching, power matching**

I. Introduction

In wideband power-matched receivers, shunt-feedback amplifiers are widely used and demonstrate low noise factor, F, and power consumption [1], [2]. However, F of wideband LNAs, such as shunt-feedback, noise-canceling, and common-gate LNAs, cannot achieve transistor minimum noise factor, F_{min}, when matched to a 50-Ω signal source. On the other hand, F of source-degenerated (SD) LNAs (SD-LNAs) can approach F_{min}, if hiqh-Q inductors are used, but such LNAs are narrowband. While in wideband SD-LNAs, filter-based designs, as in [3], achieve wideband input match, wideband simultaneous noise (i.e. $F = F_{min}$) and power matching (SNPM) is not guaranteed. This work addresses the lack of theory of designing wideband noise and power matched SD-LNAs. This theory is verified with an LNA, which was designed to replace connectorized, large, power-hungry LNAs for Cerro Chajnantor Atacama Telescope heterodyne array instrument (CHAI) [4] with an integrated LNA achieving similar noise performance.

A schematic of a cascode SD-LNA input stage driven by a signal-source Z_s and its small-signal (SS) model are shown in Fig. 1. In Fig. 1(a), it is assumed that Z_s is not necessarily equal to the characteristic impedance Z_0. "Matching Network" represents some transformation from Z_0 to Z_s. In the SS model of the SD-LNA in Fig. 1(b), the drain and gate noise currents are described by $\overline{i_{dn}^2} = 4kTB\gamma g_{do}$ and $\overline{i_{gn}^2} = 4kTB\delta\frac{\omega^2 C_{gs}^2}{5g_{d0}}$, respectively, and a correlation coefficient $c = \overline{i_{dn}i_{gn}^*}/\sqrt{\overline{i_{dn}^2}\,\overline{i_{gn}^2}}$ ($c = j0.395$ for long-channel (l.c.) MOSFETs), where γ ($\gamma = 2/3$ for l.c. MOSFETs) and δ ($\delta = 4/3$ for l.c. MOSFETs) are the excess drain- and gate-noise coefficients, respectively,

E. Zailer and L. Belostotski are with the Department of Electrical and Computer Engineering, University of Calgary, AB, T2N 1N4 Canada.

R. Plume is with the Department of Physics and Astornomy, University of Calgary, AB, T2N 1N4 Canada.

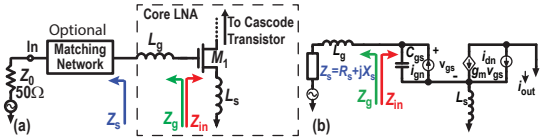

Fig. 1. (a) Schematic of the input stage of an SD-LNA and (b) its SS model. Partially correlated gate and drain noises are identified with i_{gn} and i_{dn} noise currents, and the cascode noise contribution is assumed insignificant.

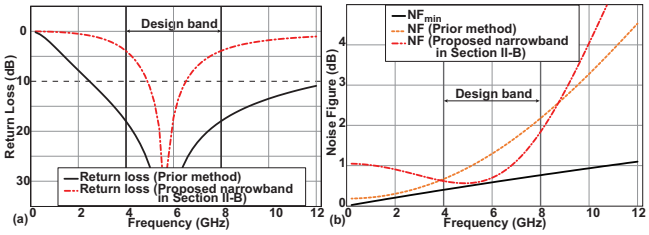

Fig. 2. SS simulations: (a) Return loss; (b) NF and NF_{min}.

and $g_{d0} = g_m/\alpha$ ($\alpha = 1$ for l.c. MOSFETs) is the output conductance when $V_{ds} = 0$, B is the noise bandwidth, k is Boltzmann's constant, and T is the absolute temperature [5], [6]. For a stand-alone M_1, the optimum admittance ($Y_{opt} = G_{opt} + jB_{opt}$) for $F = F_{min}$ depends on C_{gs} via

$$\begin{cases} G_{opt} = \omega C_{gs}\psi \overset{l.c.}{\rightarrow} 0.58\omega C_{gs} \\ B_{opt} = -\omega C_{gs}\xi \overset{l.c.}{\rightarrow} -0.75\omega C_{gs}, \end{cases} \tag{1}$$

where for brevity $\psi \equiv \alpha\sqrt{\left(1-|c|^2\right)\delta/5\gamma}$, $\xi \equiv 1 - \alpha|c|\sqrt{\delta/5\gamma}$, $\alpha = (1+0.5\rho)/(1+\rho)^2$ with $\rho \equiv V_{od}/v_{sat}L$, v_{sat} is the saturation velocity, V_{od} is the overdrive voltage, and L is the channel length [5], [6]. From the definition of α, Y_{opt} depends on V_{od} via ρ. The SD-M_1 optimum impedance for $F = F_{min}$ is $Z_{opt}^d = Y_{opt}^{-1} - sL_s$ [7] while the input impedance is $Z_{in} = R_{in} + jX_{in} = L_s g_m/C_{gs} + (sC_{gs})^{-1} + sL_s$ [5], where $L_s g_m/C_{gs} \approx \omega_T L_s$. Assuming that $Z_s = R_s$ is real, to noise match this SD-LNA (see Fig. 1(b)) $Z_g = R_s + sL_g$ should equal to Z_{opt}^d while for power matching $Z_{in} + sL_g$ should equal R_s. As $\Im\{Z_{opt}^d\} \neq \Im\{Z_{in}^*\}$, prior art [8], [9] cannot achieve SNPM using L_g, i.e. the LNA is either noise or power matched as illustrated by "Prior method" curves in Figs. 2(a) and (b). The power match bandwidth in Fig. 2(a) is wide as C_{gs} (and power consumption and circuit parasitics) is very large with methods [8], [9] at a few GHz when the lowest NF is desired. At high frequencies, smaller C_{gs} would be needed reducing power consumption and making approaches as in [9] applicable. While non-kit components, e.g., transformers [10], could be used, here,

an SD-LNA matching strategy to achieve wideband SNPM with kit components is discussed next.

II. Simultaneous noise and power matching

A. Transistor size and biasing

This work proposes a new way to find M_1 size, i.e. C_{gs}, and bias, i.e. $\alpha\,(V_{od})$, that reduce $\Delta F = F - F_{min}$ and the sensitivity, $S_f \equiv \frac{\partial \Delta F}{\partial \omega}\frac{\omega}{\Delta F}$, of ΔF to ω. We start by minimizing ΔF with respect to C_{gs}. Ignoring noise contribution from L_g and other passives at the input and with $F_{min} = 1 + 2\omega\gamma\psi/(\alpha\omega_T)$ [8], we find $\Delta F = F - F_{min} = N\left|Z_g - Z_{opt}^d\right|^2/(R_s R_{opt})$ where Lange's invariant [11] $N \equiv R_n G_{opt}$ replaces the match-variant noise resistance, R_n. It can be further shown that $N \approx \omega\gamma\psi/(\alpha\omega_T)$ since for a MOSFET $N \approx \frac{1}{2}(F_{min} - 1)$ [11]. At the resonance of C_{gs} with $L_T = L_s + L_g$ and the parameters in (1), the optimum C_{gs} from $\partial\Delta F/\partial C_{gs} = 0$ is found as

$$\omega C_{gs}^F = \frac{1}{R_s}\beta\sqrt{1 + \frac{\left(\psi^2 + \xi^2 - \xi\right)^2}{\psi^2}} \tag{2}$$

where $\beta = \psi/\left(\psi^2 + \xi^2\right)$ and where for now $X_s = 0$, i.e. $Z_s = R_s$, is assumed. For a wideband match, sensitivity S_f is zeroed with a different optimum C_{gs}, which is

$$\omega C_{gs}^S = \frac{1}{R_s}\beta. \tag{3}$$

While beyond the scope of this paper, noise due to L_g [5] can be accounted for in (2) and (3), as L_g depends on C_{gs}.

C_{gs}^F and C_{gs}^S have similar traits in their dependence on R_s^{-1} and ω. For a coincidental $\Delta F = 0$ and $S_f = 0$, $C_{gs}^F = C_{gs}^S$. This equality happens when $\psi^2 + \xi^2 = \xi$, which, through the definitions of ψ and ξ, results in $\alpha = |c|\sqrt{5\gamma/\delta} \overset{l.c.}{\to} 0.62$ and in $\beta = \psi/\xi$. With $C_{gs} = C_{gs}^S$ and regardless of α, $F = F_{min} + N\left(\psi^2 + \xi^2 + \xi\right)^2/\psi^2$ is independent of R_s. Adjusting V_{od} to set $\alpha = |c|\sqrt{5\gamma/\delta}$ makes $F = F_{min}$ *regardless* of R_s (i.e. the SNPM condition can be achieved). Note that C_{gs} may not be reduced arbitrary, which at high frequencies puts a limit on R_s.

With the apparent independence of F on R_s, (2) also makes $\partial\Delta F/\partial R_s = 0$ and the sensitivity $S_r \equiv \frac{\partial \Delta F}{\partial R_s}\frac{R_s}{\Delta F} = 0$. Now, if $X_s \neq 0$ and if $X_s + sL_T$ and $1/sC_{gs}$ resonate at a center frequency ω_0, some non-zero $\Delta X_s(\omega)$ is required for a wideband resonance of $(X_s + \Delta X_s) + sL_T$ and $1/sC_{gs}$. Then, with C_{gs} set based on (3), we find that $F = F_{min} + N\left(\Delta X_s/R_s\right)^2$, i.e. F again depends on R_s unless $R_s \to \infty$, i.e. $C_{gs} \to 0$. Since $R_s \to \infty$ is not practical, we then would like to have $\Delta X_s = 0$ while maintaining broadband match $X_s(\omega) + sL_T = -1/sC_{gs}$. Therefore, $X_s(\omega)$ must resemble a $-C$ (negative capacitor) to reduce R_s effect on F and create wideband SNPM.

B. Bandwidth consideration

When an SD-LNA in Fig. 1 is matched with L_g, the 10dB-return-loss (RL) relative bandwidth, $B_r \equiv (\omega_H - \omega_L)/\sqrt{\omega_H\omega_L}$, between low and high frequencies ω_L and ω_H, relates to the network quality factor, Q_s, by [12]

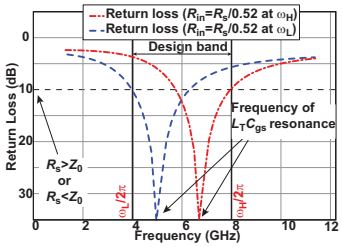

Fig. 3. Matching possibilities ($B_r = 0.54$).

$$Q_s = \frac{1}{\omega C_{gs} R_{in}} \leq \frac{2}{3B_r}. \tag{4}$$

With $C_{gs} = C_{gs}^S$, (4) results in $R_s \leq R_{in} \times 2\beta/3B_r$ giving a bandwidth-based relationship between R_s and R_{in} and differs from the conventional assumption of $R_s = R_{in}$ [3], [8], [9]. Using α from above ($\alpha = 0.62$ making $\psi = 0.36$, $\xi = 0.85$, and $\beta = 0.425$) and a 4-to-8GHz band, which is used later in an experimental example, $R_s \leq 0.4R_{in}$, which, even when assuming $\Delta X_s = 0$, results in a narrow-band design and poor RL at band edges, as confirmed in Fig. 2(a), while Fig. 2(b) shows that indeed $F = F_{min}$ is at the band center. Using $R_s \leq R_{in} \times 2\beta/3B_r$ and expressing $B_r \leq \frac{2}{3}\beta\frac{1+\Gamma}{1-\Gamma}$, where for RL$\geq$ 10 dB sets the reflection coefficient $\Gamma \equiv (R_{in} - R_s)(R_{in} + R_s) = 0.3$, shows $B_r \leq 0.54$ over which RL $\geq$ 10 dB is achieved. Such B_r makes $R_s \leq 0.52R_{in}$. For $B_r > 0.54$, a higher-order matching network is required to relax constraints in (4).

III. LNA designs and an implementation example

There are many approaches to find matching networks, provided they generate X_s, that result in wideband input resonance ($\Delta X_s = 0$) and make F independent of R_s. As 25-Ω and 100-Ω loads in a 50 Ω system result in RL≈ 10 dB, for the SD-LNA $R_s > Z_0$ or $R_s < Z_0$ could also be targeted while setting $R_{in} = R_s/0.52$ at either ω_L or ω_H as in Fig. 3. Setting $R_{in} = R_s/0.52$ at ω_H (or ω_L) and $B_r = 0.54$ results in L_g that causes L_T&C_{gs} resonance at the center frequency of B_r. This on its own results in inadequate RL at ω_L (or ω_H), as $B_r = 0.54$ is too narrow (Fig. 3). The ω_L (or ω_H) RL is rectified by using a matching network.

Many possible circuits could implement a matching strategy based on discussions above. Here, we design a matching network so that packaging and basing components, shown in Fig. 4, are reused for matching. Since these parts are already present in an SD-LNA, they do not contribute any additional noise.

We next consider four different matching strategies that result from selecting $R_s > Z_0$ or $R_s < Z_0$ and realize $R_{in} = R_s/0.52$ at ω_H or ω_L.

A. $R_s > Z_0$

Considering Fig. 5(a) and simulation results in Fig. 6, the lowpass L_1&C_1 resonates near ω_H ($Q = 1$) realizing

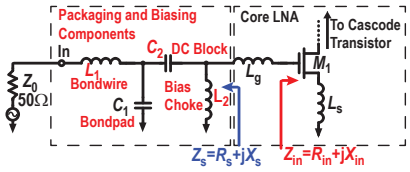

Fig. 4. Schematic of the input stage of an SD-LNA with the unavoidable packaging and biasing components.

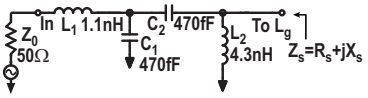

(a)

$\frac{1}{L_1C_1} = \omega_H^2$; $\frac{1}{L_2C_2} = \omega_L^2$; $\frac{1}{L_2C_1} = \omega_L^2$; $\frac{1}{L_1C_2} = \omega_H^2$;
$\Rightarrow L_1/L_2 = \omega_L^2/\omega_H^2$ and $C_1/C_2 = 1$.
When designed at ω_H: $L_s = 0.56$ nH, $L_g = 5.4$ nH, $C_{gs} = 110$ fF.
When designed at ω_L: $L_s = 1$ nH, $L_g = 12$ nH, $C_{gs} = 70$ fF.

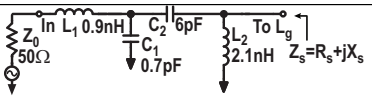

(b)

$\frac{1}{L_1C_1} = \omega_0^2$; $\frac{1}{L_2C_2} < \omega_L^2$; $\frac{1}{L_2C_1} = \omega_L^2$; $\frac{1}{L_1C_2} < \omega_L^2$;
$\Rightarrow L_1/L_2 \approx \omega_L/\omega_H$ and $C_2 \gg C_1$.
When designed at ω_H: $L_s = 0.2$ nH, $L_g = 1.8$ nH, $C_{gs} = 340$ fF.
When designed at ω_L: $L_s = 0.26$ nH, $L_g = 2.6$ nH, $C_{gs} = 250$ fF.

Fig. 5. Input matching network before L_g: (a) $R_s > Z_0$; (b) $R_s < Z_0$.

$R_s \approx 100\,\Omega$ while the highpass $L_2\&C_2$ resonates near ω_L ($Q \approx 1.7$) realizing $R_s \approx 200\,\Omega$. As R_s changes by a factor of ~2 from 4 to 8GHz, it roughly imitates $R_s \propto \omega^{-1}$ as desired for a constant C_{gs} in (3). A deviation from this behavior at the lower part of the band is not significant when $\Delta X_s \approx 0$, making $NF - NF_{min} < 0.05$ dB around the band center in Fig. 6. Since R_s can be designed at either ω_H or ω_L, both conditions are shown next where for brevity the parameters corresponding to ω_L identified in brackets. With $R_s \approx 100\,\Omega$ ($200\,\Omega$) at ω_H (ω_L), $R_{in} \approx 190\,\Omega$ ($350\,\Omega$) and $L_T\&C_{gs}$ is resonant at 6.1 GHz (5.3 GHz), which is the center frequency when $B_r = 0.54$

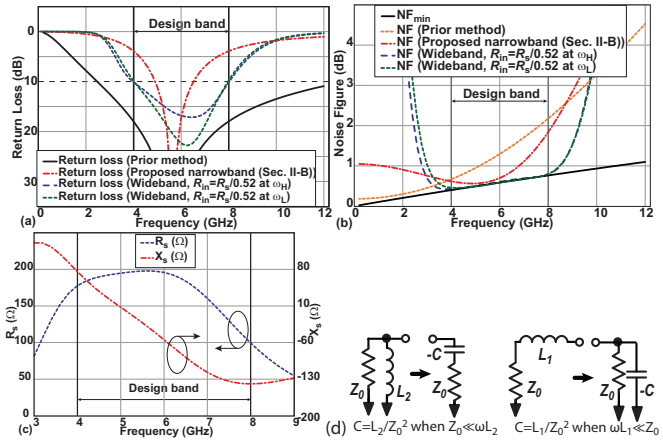

Fig. 6. $R_s > Z_0$: (a) Return loss; (b) NF and NF_{min} results from SS-model simulations. (c) $Z_s = R_s + jX_s$ realized by the matching network in top right. Ideal passives and MOSFET SS model are used in these simulations. (d) $-C$ imitation with $Z_0\&L_2$ and $Z_0\&L_1$.

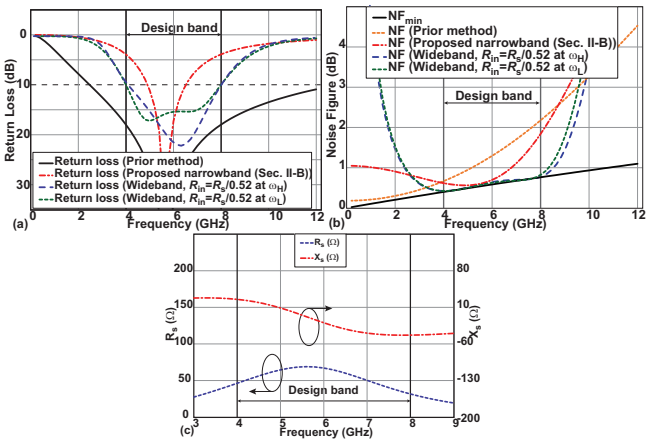

Fig. 7. $R_s < Z_0$: (a) Return loss; (b) NF and NF_{min} results from SS-model simulations. (c) $Z_s = R_s + jX_s$ realized by the matching network in top right. Ideal passives and MOSFET SS model are used in these simulations.

and $\omega_H = 2\pi \times 8$ GHz ($\omega_L = 2\pi \times 4$ GHz). The parallel resonance of $C_1\&L_2$ near ω_L and the series resonance of $L_1\&C_2$ near ω_H also ensure $-C$-like behavior (explained in Fig. 6(d)) for X_s, thus making $\Delta X_s \approx 0$ above and below 6.1 GHz (5.3 GHz), as assumed when deriving (2) and (3).

B. $R_s < Z_0$

Considering the matching network in Fig. 5(b) and simulation results in Fig. 7, $L_2\&C_1$ resonates near ω_L ($Q \approx 0.9$), while together with $L_1\&Z_0$ imitating $-C$ behavior. $L_1\&C_1$ resonates near ω_0 ($Q \approx 0.7$), while R_s varies from $50\,\Omega$ at ω_L to $30\,\Omega$ at ω_H due to the $L_1\&L_2$ divider to imitate the reduction of R_s with ω. Again, R_s can be set at either ω_L or ω_H, with results related to ω_H shown in brackets. With $R_s \approx 50\,\Omega$ ($30\,\Omega$) at ω_L (ω_H), $R_{in} \approx 95\,\Omega$ ($60\,\Omega$) and $L_T\&C_{gs}$ is resonant at 5.4 GHz (6.1 GHz), which is the center frequency when $B_r = 0.54$ and $\omega_L = 2\pi \times 4$ GHz ($\omega_H = 2\pi \times 8$ GHz). For input resonance $X_s(\omega) + sL_T = -1/sC_{gs}$, $L_1\&Z_0$ and $L_2\&Z_0$ approximate $-C$ behavior as in Fig. 6(d).

In contrast to $R_{in} \approx \omega_T L_s$, the core-LNA voltage gain $G \propto L_s^{-1}$ requires a compromise with B_r through (4). Advantageously, this packaging/biasing network has enough elements to accommodate some flexibility.

C. Experimental example

Out of the possible design options, $R_s < Z_0$ with $R_{in} = R_s/0.52$ at ω_H was selected for implementation as it resulted in the smallest $L_s = 0.2\,nH$ and $L_g = 1.8\,nH$ at the expense of larger power consumption. The lowest power design would be with $R_s > Z_0$ with $R_{in} = R_s/0.52$ at ω_L, but, with $L_s = 1\,nH$ and $L_g = 12\,nH$.

A 4-to-8 GHz SD-LNA, with its schematic in Fig. 8, was implemented in 0.13-μm CMOS. As a part of a larger system, the LNA is followed by 2 differential stages. Due to the flexibility in designing the input network and selecting R_s, the design started by (a) selecting the kit inductor

This article has been accepted for publication in a future issue of this journal, but has not been fully edited. Content may change prior to final publication. Citation information: DOI 10.1109/LSSC.2020.2986645, IEEE Solid-State Circuits Letters

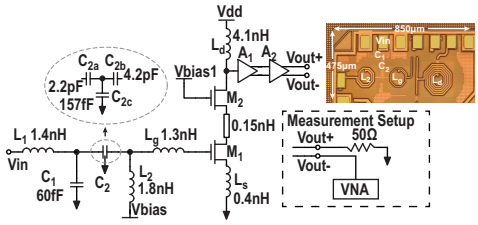

Fig. 8. Schematic of die photo the implemented circuit with C_1 being a padded bondpad capacitance.

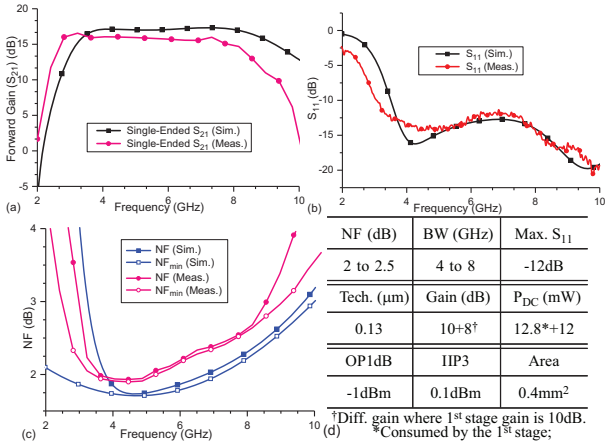

NF (dB)	BW (GHz)	Max. S_{11}
2 to 2.5	4 to 8	-12dB
Tech. (μm)	Gain (dB)	P_{DC} (mW)
0.13	10+8†	12.8*+12
OP1dB	IIP3	Area
-1dBm	0.1dBm	0.4mm²

†Diff. gain where 1st stage gain is 10dB.
*Consumed by the 1st stage;
(d)

Fig. 9. Simulation and measurement of (a) S_{21}, (b) S_{11}, (c) NF. (d) Performance summary.

with the highest Q in-band for L_g; (b) selecting a high-Q kit inductor L_2; and (c) targeting RL $\geq$ 12 dB. With this L_g, the requirement for resonance at 6.1 GHz sets the gate capacitance, which sets the required R_s from (3) at ω_H and the matching network to realize R_s. Accounting for layout parasitics gives the components in Fig. 8. In the final circuit, $C_{gs} \approx 150$ fF, $V_{od} = 0.23$ V, and $\alpha \approx 0.63$.

Noise and S-parameter were measured in a single-ended mode with the LNA 2nd terminal loaded as in Fig. 8. Such measurements do not impact the NF, but the measured gain is 3 dB lower than in the intended differential mode. The test results in Fig. 9 show that in the 4-to-8 GHz band the LNA has a maximum NF of 2.5 dB, differential-output gain of 18 dB, and RL $>$ 12 dB. The LNA NF and NF_{min} are within 2.8% over the full band indicating wideband noise matching and are only slightly higher than in the post-layout simulations. The LNA consumes 24.8 mW from a 1.6 V supply, of which the front-stage LNA consumes 12.8 mW. Fig. 10 shows how the described LNA compares to other 0.13-μm CMOS LNAs [13].

IV. Conclusion

This work presented a way of noise and power matching SD-LNAs. This strategy is based on reducing $\Delta F = F - F_{min}$ and the sensitivity of ΔF to frequency, ω. Unlike other SD-LNA design strategies, in this work (a) the C_{gs} that minimizes noise-factor penalty ΔF and the sensitivity, S_f, of ΔF to frequency is found; (b) the overdrive voltage, V_{od}, for coincidental $\Delta F = 0$ and $S_f = 0$

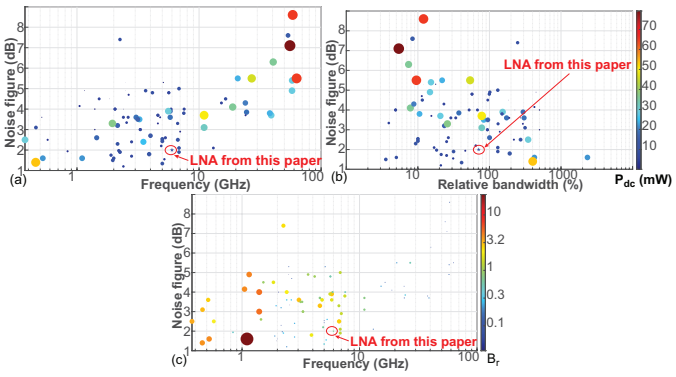

Fig. 10. Performances of 0.13-μm CMOS LNAs published since 2000 [13]. Larger markers of brigher colors indicate higher dc power in (a) and (b) and larger B_r in (c).

is found; (c) these C_{gs} and V_{od} result in noise figure, NF, being independent of the signal-source impedance $Z_s = R_s + jX_s$ for SNPM; (d) the input resistance, R_{in}, is not constrained to 50 Ω; (e) the effect of reactive mismatch on ΔF is minimized with small C_{gs}; and (f) Z_s with ω^{-1} dependence is synthesized with the biasing and packaging components to achieve SNPM without additional noise. An experimental example demonstrated the ability of this approach to maintain ΔF within 2.8% of F_{min} from 4 to 8 GHz while achieving >12-dB return loss in band.

References

[1] Y. Lin *et al.*, "High-performance wideband low-noise amplifier using enhanced π-match input network," *IEEE Microw. Wireless Comp. Lett.*, vol. 24, no. 3, pp. 200–202, March 2014.

[2] P. Chang and S. S. H. Hsu, "A compact 0.1-14-GHz ultra-wideband low-noise amplifier in 0.13-μm cmos," *IEEE Trans. Microw. Theory Techn.*, vol. 58, no. 10, pp. 2575–2581, Oct 2010.

[3] A. Bevilacqua and A. M. Niknejad, "An ultrawideband CMOS low-noise amplifier for 3.1-10.6-GHz wireless receivers," *IEEE J. Solid-State Circuits*, vol. 39, no. 12, pp. 2259–2268, Dec 2004.

[4] E. Zailer *et al.*, "University of calgary participation in ccat chai development," in *IEEE Int. Symp. Ant. Propag./URSI Nat. Radio Science Meet.*, July 2015, pp. 1378–1379.

[5] L. Belostotski and J. W. Haslett, "Noise figure optimization of inductively degenerated CMOS LNAs with integrated gate inductors," *IEEE Trans. Circuits Syst. I*, vol. 53, no. 7, pp. 1409–1422, July 2006.

[6] T. H. Lee, *The Design of CMOS Radio-Frequency Integrated Circuits*, 2nd, Ed. New York: Cambridge Univeristy Press, 2004.

[7] L. Belostotski and J. W. Haslett, "Two-port noise figure optimization of source-degenerated cascode CMOS LNAs," *Analog Integ. Circ. Sign. Proces.*, vol. 55, no. 2, pp. 125–137, May 2008.

[8] D. K. Shaeffer and T. H. Lee, "A 1.5-V, 1.5-GHz CMOS low noise amplifier," *IEEE J. Solid-State Circuits*, vol. 32, no. 5, pp. 745–759, May 1997.

[9] S. T. Nicolson and S. P. Voinigescu, "Methodology for simultaneous noise and impedance matching in W-band LNAs," in *IEEE CSICS*, Nov. 2006, pp. 279–282.

[10] M. T. Reiha and J. R. Long, "A 1.2 V reactive-feedback 3.1-10.6 GHz low-noise amplifier in 0.13 μm CMOS," *IEEE J. of Solid-State Circuits*, vol. 42, no. 5, pp. 1023–1033, May 2007.

[11] L. Belostotski, "On the number of noise parameters for analyses of circuits with MOSFETs," *IEEE Trans. Microw. Theory Techn.*, vol. 59, no. 4, pp. 877–881, April 2011.

[12] L. Belostotski and J. W. Haslett, "Noise figure optimization of wide-band inductively-degenerated CMOS LNAs," in *IEEE MSCAS*, Montreal, Canada, 5-8 August 2007, pp. 1002–1005.

[13] L. Belostotski *et al.* Low-noise-amplifier (LNA) performance survey. [Online]. Available: https://www.ucalgary.ca/lbelosto